INTERNATIONAL ATOMIC ENERGY AGENCY
UNITED NATIONS EDUCATIONAL, SCIENTIFIC AND CULTURAL ORGANIZATION

INTERNATIONAL CENTRE FOR THEORETICAL PHYSICS
34100 TRIESTE (ITALY) - P.O.B. 586 - MIRAMARE - STRADA COSTIERA 11 - TELEPHONE: 2240-1
CABLE: CENTRATOM - TELEX 460392-1

SMR/455 - 16

EXPERIMENTAL WORKSHOP ON HIGH TEMPERATURE SUPERCONDUCTORS & RELATED MATERIALS (BASIC ACTIVITIES)

12 - 30 MARCH 1990

MAGNETIC AND TRANSPORT PROPERTIES OF HIGH T_c SUPERCONDUCTORS

FRANCISCO DE LA CRUZ

Comision Nacional de Energia Atomica
Centro Atomico Bariloche
8400 Bariloche
Argentina

TRIESTE MARCH 1990

MAGNETIC AND TRANSPORT PROPERTIES OF HIGH Tc SUPERCONDUCTORS

F. de la Cruz

Centro Atómico Bariloche

8400 S.C. de Bariloche, Rio Negro, Argentina

The experimental results on which we base the understanding of the magnetic properties were obtained in:

POLYCRYSTALS (Ceramics) $La_{1.8}Sr_{0.2}CuO_{4-\delta}$

SINGLE CRYSTALS $YBa_2Cu_3O_{7-\delta}$

Is the distinction important?

We will begin the lectures studying the results obtained in ceramics. We will see that the magnetic response is typical of granular superconductors.

The first suggestion came from K.A. Müller et al., Phys. Rev. Lett. 58, 1143 (1987). Müller et al. thought of the granularity as an intrinsic property.

Today we do not believe it is intrinsic but rather, a quite peculiar property of the defects of the oxide ceramics (not necessarily high Tc superconductors).

The picture we discuss is a result of the analysis of many experiments. The data I will use has been obtained in the Low Temperature Group at Bariloche.

I.- Definition of Granularity

In the context of these lectures the definition of a granular system follows from fig. 1: Superconducting islands separated by a non-superconducting matrix. Notice that the superconducting material does not percolate. The non-superconducting matrix builds up a multiple connected system.

The granularity defined here is different from that observed in metallic composites. See Abeles, Applied Solid State Physics, Vol. 6 (1976).

First we discuss what we expect from a system like this and, afterwards, we compare this expectation with experimental results.

We assume that the non-superconducting material is an insulator.

II.- Necessary conditions to Build a Granular System

a) Decoupling between metallic regions.

b) Multiple connected insulating regions.

The model is just a "tunneling" model, coupling the electronic properties of the metal, represented by the eigenfunctions ψ_i, ψ_j associated to the interconnected regions i, j. In the case of the normal state ψ_i, ψ_j represent the wave functions of the normal electrons. In the superconducting state they are the solutions of the G-L equations for the islands i and j.

This type of model has been used for many years to represent the behaviour of inhomogeneous materials artificially designed.

What is interesting and surprising is that the oxide ceramics show in a natural way such a behaviour.

The point we emphasize here is that the ceramic system should

not be taken as an heretogeneous material with superconducting and normal properties determined by the parallel and series combination of the corresponding constituents. As far as $H_{ij} \neq 0$ those properties are determined by the quantum transfer of particles from different islands. From this point of view the superconducting and transport properties will be those of a material where the insulating matrix only determines the intensity of the elastic transfer of particles.

Two theoretical papers have been recently published in relation to granular models applied to high Tc ceramics: J.R. Clem, Physica C 153, 50 (1988), M. Tinkham and C.J. Lobb, Solid State Physics Vol. 42.

A comprehensive critical review of the experimental data up to 1988 can be found in A.P. Malozemoff, Physical Properties of High Temperature Superconductors, Ed. D.M. Ginsberg (World Scientific Publishing Co., Singapore, 1989.

III.- Expected Superconducting Phase Diagram

A scheme of the expected phase diagram is shown in figure 2.

I Full Meissner state. Locked phase among islands.

II Fluxons between islands that remain in the Meissner state.

III Almost isolated superconducting islands in the Meissner state.

II' Coexistence of fluxons and vortices.

IV Vortices within the islands.

V Reversibility region. Not expected, but characteristical of the ceramic superconductors.

VI Normal state.

In the diagram there are two temperatures indicated, T_{CG} T_{CL}. The first one indicates the superconducting nucleation in the grains, the second the phase lock temperature between grains.

IV.- Experimental Evidence

Figure 3 shows the electrical resistance, $\rho(T)$, as a function of temperature of $La_{1.8}Sr_{0.2}CuO_{4-\delta}$ for different oxygen content, E. Osquiguil et al., Phys. Rev. B 38, 2840 (1988). Notice that the oxygen concentration changes the temperature dependence of $\rho(T)$ and the superconducting transition width, leaving constant the onset temperature T_{CG}. In principle we can think that T_{CG} is the island critical temperature and T_{CL} the temperature where $\rho(T) = 0$. However, we can also argue that $T_{CO} - T_{CL} = \Delta T$ is just a transition width.

Let us see what we obtain from flux expulsion measurements. Figure 4 shows $\phi(T)/\phi_N = f(T)$, for zero field cooling (ZFC) experiments.

$\phi(T) = \int h(r) d^2r$ = magnetic flux

$\phi_N = H_a . A$ A=area of the sample

In figure 5 we plot $\frac{\phi(T = 1.5K)}{\phi_N} = f(H)$ for an oxygenated sample. Notice the two plateaus, indicating that $\frac{B}{H} = C$ (the constant is the ratio of two areas). For $H \to 0$ $C \simeq 1$, for $H \simeq 10$ Oe $C \simeq 0.6$.

$B \simeq H$ is a condition of the Meissner state. We can imagine again that the plateaus correspond to a full Meissner state in the whole sample at lower fields and to a Meissner state in the islands at higher fields, in agreement with the granular model. The behavior shown in fig. 5 is in agreement with what can be

expected from fig. 2.

Let us see the equivalent data corresponding to a deoxygenated material. This is seen in figs. 6 and 7. Again, two plateaus, but now not very well defined and the expulsion remains always far from total expulsion. This is again in agreement with the granular picture with islands interconnected by a weaker H_{ij}.

But, can we prove that we have islands with a single T_{CO} and a single percolation temperature? The answer is yes.

To prove it we will use remanent magnetic moment measurements. In this context the remanent moment, RM, is obtained by decreasing to zero the magnetic field, after being applied in a ZFC, or field cooling experiments. Up to now all the magnetic measurements we have discussed were obtained in ZFC experiments.

Assuming the granular picture is correct the phase diagram of our material should correspond to some of the cases indicated in fig. 2. We concentrate our attention on the picture corresponding to regions II and II'. Making ZFC measurements we should be able to detect H_{c1}^{G} (lower critical field of the grains), F. de la Cruz et al. in Progress in High Tc Superconductivity, ed. by R. Nicolsky, R.A. Barrio, O. Ferreira and R. Escudero. (Proc. of the First Latin American Conference on High Tc Superconductivity, World Scientific Publ. Co., Singapore, Vol. 9, 5 (1988)) and L. Civale et al. Mod. Phys. Lett. B 3, 173 (1989). If the applied field has surpassed the lower critical field of the phase locked state but is kept below H_{c1}^{G}, the remanent moment at H = 0 should tend to zero at T_{CL}. On the contrary, if the applied field has crossed the $H_{c1}^{G}(T)$ line the remanent moment should disappear at T_{CG}. In this way we have been able to determine the experimental

$H_{c1}^{G}(T)$ for the oxygenated and deoxygenated materials, see figs. 8 and 9. The result is important, it says that there is no transition width due to inhomogeneous material but a transition width due to thermal phase fluctuations. This is an interesting conclusion, to be discussed as a problem.

V.- Low Field Results

The phase diagrams of figs. 8 and 9 has no region I. This is an interesting problem we must analyze, to show how to use the experimental techniques to determine the phase diagram.

When discussing figures 5 and 7 we have said that the low field plateau was a necessary condition to observe a Meissner effect, B = C H. We measure the magnetic flux through the sample, using a SQUID.

$$\phi = \int h(r)\, d^2 r$$

The sample is a slab of thickness d and width w. If the sample is in the Meissner state.

$$h(x) = H_a\, e^{-x/\lambda}$$

With this field distribution and $d \gg \lambda(o)$

$$\phi = (2\lambda(T).P)\, H_a, \qquad P = 2(w+d)$$

Since $\lambda(T)$ is a length characteristic of a thermodynamic state, representing the minimum Gibbs energy, $\phi(T)$ has to be reversible in temperature. As a consequence, $\phi(T,H)$ is

proportional to H and reversible in T and H. Precise measurements at very low fields demonstrated that this was not the case, see fig. 10.

VI. Critical State

Once proved that the sample is not in the Meissner state, we conclude that even the lowest field of 0.01 Oe used in the ZFC measurements is large enough to overcome the low critical field of the granular system. Let us see if the sample responds to the characteristics of region II. We know from the RM experiments that there is a finite flux pinning. To describe the pinning we use the most simple model of the critical state; C.P. Bean, Phys. Rev. Lett. 8, 250 (1962) and L. Civale et al. Solid State Commun. 65, 129 (1988).

$$\frac{dh}{dx} = \frac{4\pi}{c} J_c$$

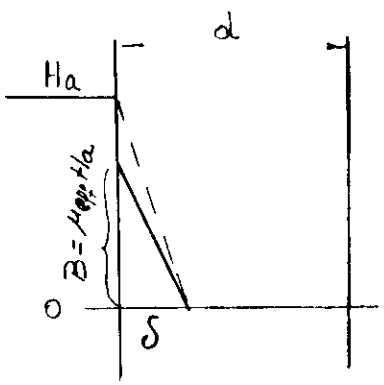

J_c is assumed to be independent of h. We assume that the applied field $H_a >> H_{c1}$. In this way the only critical relevant currents are the transport or critical currents. That is, we disregard the manetization of the material. We see from the figure that $\delta \sim \frac{cH_a}{4\pi J_c}$. The flux for a slab of perimeter P is essentially $\phi = \frac{1}{2} H_a \delta (2W+2d)$, as a consequence $\phi = \frac{C}{8\pi} \frac{(2W+2d)}{J_c} H_a^2$. Then, ϕ is, in the critical state, proportional to H_a^2. This can be a good approximation as far as $\delta < \frac{d}{2}$. You can calculate what

happens once $\delta = \frac{d}{2}$. That is, once $H_a \geq H_s(d,T)$ you will find:

$$\phi = A \left(H_a - \frac{H_s}{2}\right)$$

indicating that ϕ is proportional to H_a.

This is the Bean model for a homogeneous material. We have to generalize it for a granular system.

In region II the islands are in the Meissner state. This indicates that the transport currents are flowing between grains and on the surface of the grains in a thickness λ_c. To take into account the Meissner contribution of the island we introduce $B = \mu_{eff} H_a$. The permeability, μ_{eff}, represents the fraction of the sample in the Meissner state when the intergranular currents are zero. With these modifications

$$\phi = \frac{C}{8\pi} \frac{P}{J_c} \mu_{eff} H_a^2 \qquad H_a < H_s$$

$$\phi = \mu_{eff} A \left[H_a - \frac{H_s}{2}\right] \qquad H_a > H_s$$

Using an expanded scale for the results of fig. 5 we find what is shown in figs. 11 and 12.

Since the results indicate that the generalization of the Bean model permits to understand the flux dependence on field, we should now think which is the characteristic length of the problem, allowing for the use of the macroscopic picture. We know that we are disregarding the Meissner currents. As a consequence, the experimental results could be valid if $H_a >> H_{c1}^L$ or, what is the same, $\delta >> \lambda_L$. Careful measurements at H→0 show deviation from

Bean model as indicated in fig. 13. Bean model is a macroscopic model, disregading fine magnetic structures. That means that the scale to define h(T) has to be large compared to the size of the superconducting islands, a that is $\delta >> a$. Since figures 11 and 12 show the validity of the Bean model we can use the data to determine μ_{eff} and J_c. The value of $J_c \simeq 100$ amp/cm^2 at $T \simeq 0$ for the oxygenated material is in good agreement with the value obtained from transport measurements. The corresponding permeability is $\mu_{eff} \simeq 0.6$. These are the two macroscopic parameters of the model.

VII.- Meissner Effect

As we have already discussed, the lowest fields used in the ZFC experiments were too large compared to H_{c1}^{G}. On the other hand the deviations from Bean model, shown in fig. 13, indicate that the lowest field accessible in the experiments is rather close to $H_{c1}(0)$. As a consequence we can attribute the flux penetration at the lowest measuring field to the Meissner penetration. Taking into account the granular structure through the defined effective permeability we have

$$\frac{\phi}{\phi_N} = \mu_{eff} \frac{4\lambda_L(T)}{d}$$

where it is assumed $w >> d$. Using the experimental flux expulsion for the oxygenated material we obtain $\lambda_L(T=1.4) \simeq 40\mu m$. Following the papers of Clem and/or Tinkham $H_{c1}(T) = \frac{\phi_o}{4\pi\lambda_L(T)}$. Using the experimentally obtained λ_L we have $H_{c1}(T=1.4) \simeq 6$mOe. This result indicates the consistency of the assumptions made to calculate λ_L.

The penetration depth, λ_L, is extremely large in a granular system due to the weak shielding capability of the Josephson junctions. Following Tinkham

$$\lambda_L(T) = \left[\frac{c\phi_o}{8\pi^2 a J_c(T)\mu_{eff}}\right]^{1/2}$$

where a is the average diameter of the superconducting islands. Since we have experimentally determined λ_L, J_c and μ_{eff} we can calculate a. Using the experimental data for the oxygenated material we obtain $a \simeq 1.7\mu m$. We have determined all the important parameters of the granular system. We can make another experiment to show the consistency of the results. Region III in the phase diagram represents a magnetic state characterized by a collection of isolated superconducting islands. The temperature dependence of the flux expulsion is determined by the Meissner state of islands of finite size ($2\mu m$ diameter). The results are shown in fig. 14.

VIII.- Meissner State of the Superconducting Islands

The temperature dependence of the ZFC flux expulsion shown in fig. 14 is broad, scales with field and is fairly temperature reversible. Assuming that the superconducting islands are spheres of radius R, the flux in the ceramic sample can be expressed by

$$\phi = A\, H_a \left[1 - \frac{3}{2}\,\eta\, g\left(R/\lambda_c\right)\right]$$

$\eta = V_{esf}/V$ is the ratio of the volume occupied by the spheres to the sample volume and

$$g\left(R/\lambda\right) = \left[1 - \frac{3\lambda}{R}\coth\frac{R}{\lambda} + 3\frac{\lambda^2}{R^2}\right]$$

Assuming $\lambda = \lambda(0)(1-t^4)^{-1/2}$ we fit the experimental data with the formula indicated above. The results of the fitting is shown in fig. 14. The free parameters, η and $\frac{R}{\lambda}$, are determined by the fitting. We obtain $R/\lambda(o) = 3.2$ and $\eta = 0.81$. The value of η indicates that 80% of the sample volume is filled by the superconducting islands. This should be taken as a lower limit since the island with smaller diameter contribute less to the magnetic signal. The type of measurements shown in fig. 14 allows the determination of H_{C1}^{G}. In that figure the vortices are seen to penetrate into the sample at 27K. Using this definition of $H_{C1}(T)$ we plot the results in fig. 15. From $H_{C1} = \frac{\phi_o}{4\pi\lambda_G(T)}$ the penetration depth of the grains are obtained $\lambda_G(o) = 3.000\text{Å}$. With this value and the R/λ obtained before we have $2R = 1.7\ \mu m$, in excellent agreement with the value deduced from $\lambda_L(o)$ in an independent measurement.

I believe these results are good enough to demonstrate the granularity behavior of the ceramic. It also shows that once the granular behaviour is accepted the experimental data can be used to learn about the inter and intragranular properties. The changes induced by the oxygen concentration in the granular system are of particular interest. The oxygen concentration tunesthe characteristics of the barriers between the superconducting islands and, eventually, determines the size of the superconducting islands.

IX.- Conclusions

We have no more time to devote to this topic. I will mention some conclusions we have reached from the investigation of the granularity in ceramic systems.

1) Superconductivity in ceramics has a granular behavior. The size of the superconducting grains is much smaller than the ceramic grains.
2) A necessary condition for granularity is the small coherence length of the superconducting material but this is not a sufficient condition. The granularity, as observed in these materials, requires the existence of multiple connected "two dimensional" regions of thickness of the order of ξ and a surface per grain of the order or larger than λ^2.
3) The origin and nature of the insulating matrix is unknown. However, the oxygen vacancies have an important role in determining the intensity of the Josephson coupling and, eventually, in determining the size of the superconducting grains. The results indicate that oxygen vacancies induce a highly correlated distribution of defects.
4) The granular picture has direct implications in the behaviour and understanding of the transport properties in the normal state. The insulating barriers between islands are Josephson barriers for superconducting pairs and particle potential barriers in the normal state. This scheme allows us to understand the transport properties as those corresponding to a homogeneous system, where part of the elastic scattering is due to quantum tunneling between islands. In this way the measurement of the resistivity provides information on the bulk behavior of a single material and is not the response of

two different carriers acting in series and parallel circuits.

Magnetic Response of Single Crystals

In these lectures we will discuss some aspects of the magnetic behavior of high Tc single crystals. The information I will provide is much more concentrated in particular topics than what we have already discussed in ceramics. I provide some general references, that can be of interest to the participants.

- A.P. Malozenoff, in "Physical Properties of High Temperature Superconductors - I" ed., D.M. Ginsberg, World Scientific, Singapore (1989).
- P.L. Gammel, L.F. Schneemeyer, J.V. Waszczak, and D.J. Bishop, Phys. Rev. Lett., 61, 1666 (1988).
- T.T.M. Palstra, B. Batlogg, R.B. Van Dover, L.F. Schneemeyer and J.V. Waszczak, Phys. Rev. Lett. 61, 1662 (1988).
- M.P.A. Fisher, Phys. Rev. Letts. 62, 1415 (1989).
- D.R. Nelson, Phys. Rev. Letts. 60, 1973 (1988).
- D.R. Nelson and H. Sebastian Seung, preprint.
- A. Houghton, R.A. Pelcovits and A. Sudbo, preprint (1989).
- H. Safar, H. Pastoriza, J. Guimpel, F. de la Cruz, D.J. Bishop, L.F. Schneemeyer and J.V. Waszczak, preprint.
- S. Doniach, preprint.

The activity in this area is quite intense. From my point of view, the magnetic response of these materials is one of the most exciting aspects of the new superconductivity. From a basic point of view the interest is concentrated in the discussion of the equilibrium state of the superconducting material, when vortices are induced by the presence of an external magnetic field.

In the old superconductivity we are used to thinking of the three dimensional vortex lattice as a system where the equilibrium state is determined by the minimum internal energy. In this interpretation the vortices are considered as flux interacting magnetic lines with no entropy. The disorder in the lattice is introduced only by topological defects. The effect of disorder has been discussed in a paper by A.I. Larkin and Yu. N. Ovchinnikov, Journal of Low Temperature Physics 34, 409 (1979). I believe that discussion is an excellent introduction to the necessary extensions for the new superconductors.

The existence of a reversibility line in the phase diagram was remarked by K.A. Müller et al., Phys. Rev. Lett. 58, 1143 (1987). This reversibility line has been interpreted in different ways: a giant flux creep based on a traditional behavior is suggested by Y. Yeshurun and A.P. Malozenoff, Phys. Rev. Lett. 60, 2202 (1988) while a melting of the vortex lattice is suggested by Gammel et al., Phys. Ref. Lett. 61, 1666 (1988). Different theoretical interpretation can be found in the references provided at the beginning of this chapter.

In this lecture I will discuss some experiments done in Bariloche related to the behavior of the vortices of the high Tc oxide superconductors.

I.- Experimental Set-Up

We have used a SQUID magnetometer together with a custom made cryostat to measure the Meissner state of YBaCuO single crystals, provided by AT and T Bell Labs. The main characteristic of the cryostat is the low magnetic background in the range of temperatures of interest. The magnetic background signal is of the order of five flux quanta per Oe in the range from 1K to 100K.

The high quality of the crystal can be seen in fig. 1 where the FC and ZFC flux penetration fraction, ϕ/ϕ_N, as a function of temperature is plotted. The reversibility of the temperature dependence of the flux expulsion is evident. The reversibility is lost at higher fields where the F.C. experiments show a large fraction of flux trapping.

II.- Low Field Expulsion

The zero field cooling experiments show reversibility, (see fig. 1') up to a well defined temperature, determined by the applied magnetic field. At that temperature, Tc1(H), flux rapidly penetrates into the sample and, at higher temperatures, flux irreversibility is evident.

From measurements as those shown in fig. 1' we can obtain Tc1(H). The results are plotted in fig. 2.

III.- Low Critical Field

The experiments were done with the applied field parallel and perpendicular to the Cu-O planes. In the inset of fig. 2 we see the results for both orientations, where corrections due to the demagnetization factor are taken into account only in the perpendicular case.

We will not discuss here why we believe the Hc1(T) shown in fig. 2 corresponds to the ideal low critical field of the YBaCuO. The low temperature critical field data coincides with those reported by Krusin-Elbaum et al., Phys. Rev. B 39, 2903 (1989), except at high temperatures where we observe a well defined collapse of Hc1(T). On the contrary in the work by Krusin-Elbaum et al, the Hc1(T) is found to be linear up to Tc. We have no explanation for the discrepancy but our results have been reproduced in four different single crystals.

In our opinion the result is intrinsic and important for future interpretation of the microscopic and macroscopic properties of the high Tc superconductors.

IV.- Speculations

We can only speculate on the origin of the low field transition previously indicated. It is important to notice that the collapse of Hc1(T) is induced at a well defined temperature for both field directions, indicating that the transition is not induced by magnetic energy but by thermal energy.

Several authors (de Jong, preprint, Friedel, preprint, Malozemoff et al, Conf. on High Temp. Supercond. mat., Stanford 1989, Doniach, preprint), have suggested that the bulk superconductivity in the high Tc material is due to Josephson-like coupling between stacks of Cu-O layers. The idea is based on the existence of a coupling energy Ej between the superconducting "two dimensional" layers nucleated at the Cu-O stacks. If this is accepted, a loss of phase coherence among the Cu-O stacks should be expected at $kT^* = Ej$. Once the phase fluctuates in space, currents are induced and the Meissner state is precluded.

From a phenomenological point of view it is easier to understand the field penetration in the parallel direction. One might think that the penetration in the perpendicular direction will take place in a mean field $H_{c1}(T)$, thus the energy is minimized for straight vortices magnetically coupled between CuO stacks. On the other hand vortices will be straight vortices only if the entropy is diregarded. The phase fluctuation between Cu-O stacks induces currents perpendicular to those stacks. The thermal energy induces a non straight behavior of the vortices, introducing entropy to the magneticsystem. In this case the vortices will look like the one shown in fig. 3. In this case, the distribution and nucleation of vortices will be determined by the minimum of the Gibbs energy and not by the minimum of the internal energy. In another context similar drawings of the perpendicular vortices can be found in a recent paper by Doniach (preprint).

Once the drop of $H_{c1}(T)$ at T^* is accepted it is reasonable to ask whether this transition is related to the "reversibility" or "melting" line. As a consequence, we started experiments using the SQUID magnetometer and mechanical oscillators to determined the behaviour of those lines near T^* and up to Tc. At the moment we have only preliminary data but we can say that the "melting" line in YBaCuO with H perpendicular to the Cu-O planes has a noticeable curvature t low fields with a clear extrapolation towards Tc (C. Durán et al., private commun.). The "reversibility" line as measured with the SQUID also extrapolates to Tc (H. Safar et al., private commun.). On the other hand F.C. measurements indicate a clear change in the vortex dynamics in another almost vertical

line in the phase diagram, starting at T^* (H. Safar, et al., private communication).

Figure 4 shows some preliminary results indicating the present stage of the investigation of the phase diagram at low fields.

Magnetic Properties

Polycrystals La-Sr-Cu-O

Simple Gystals Y.BaCuO

Based in experiments made in

Bariloche

L Civale	SQUID
H Zapar	Resistivity
J Guimpel	Mechanical oscillator
E Osquiguil	
R Decca	D. Bishop
C Duran	L. F. Schneemeyer
H. Pastoriza	J.V. Wasaccak

Granularity

Reversibility Line

Thermal Induced Two Dimensional Decoupling

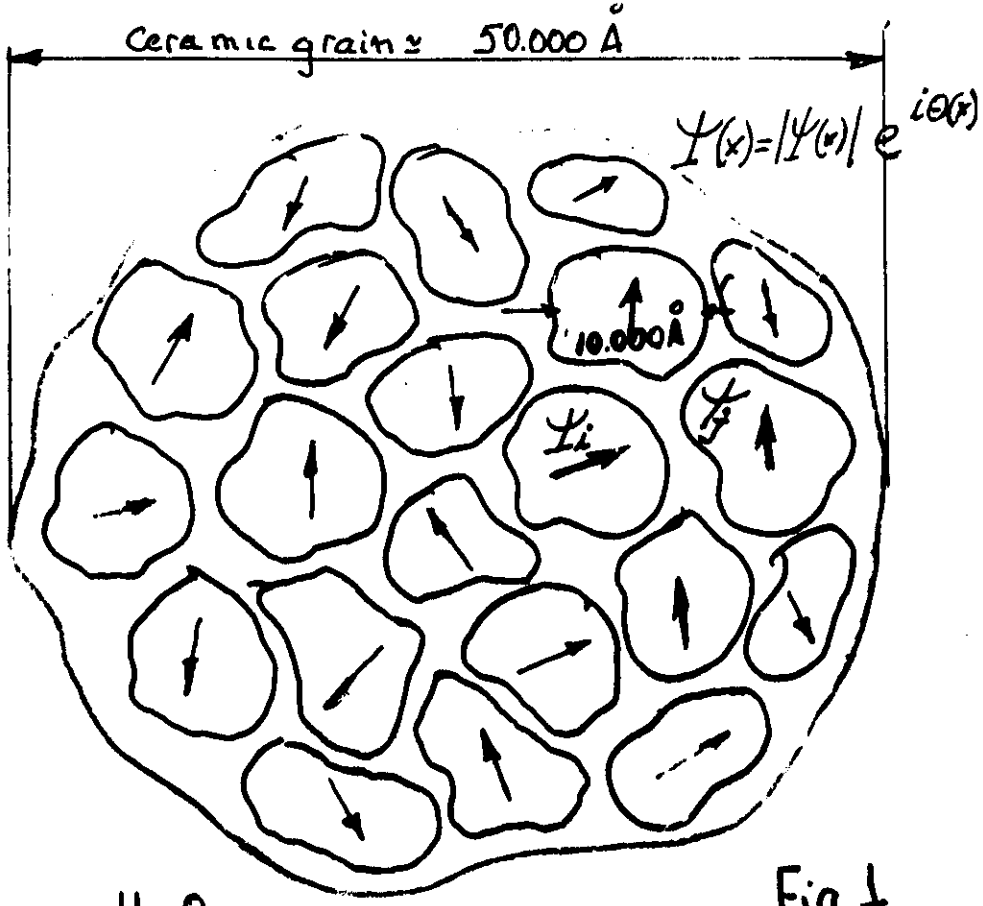

Fig 1

H=0

coherence within the islands

no coherence between islands

$J \neq 0$

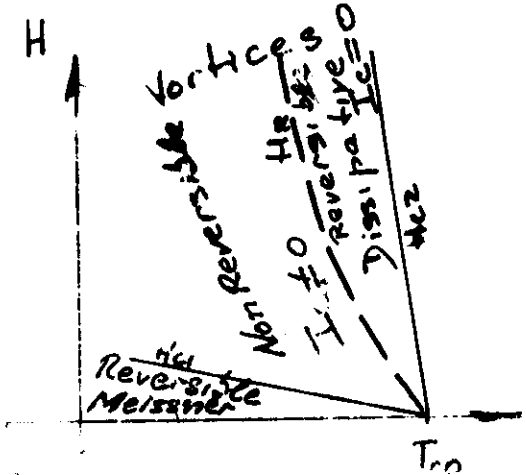

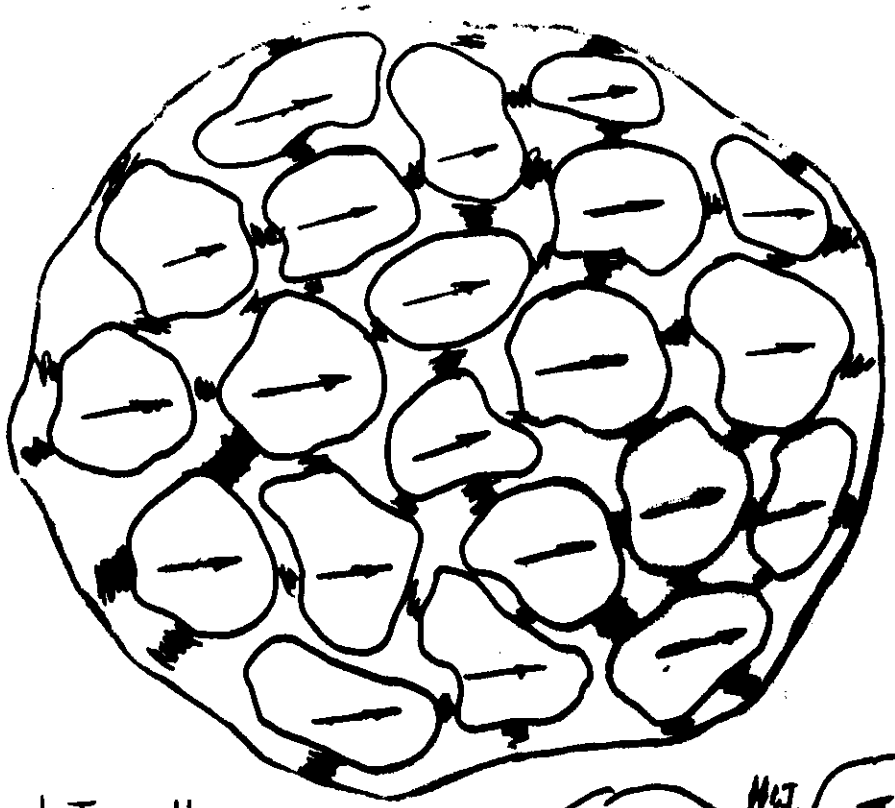

$kT_c \simeq H_{ij}$

$T < T_c$ $H=0$: Coherent state

$T_c < T < T_{co}$ phase Fluctation

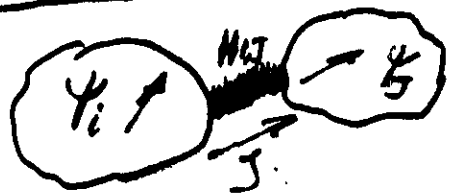

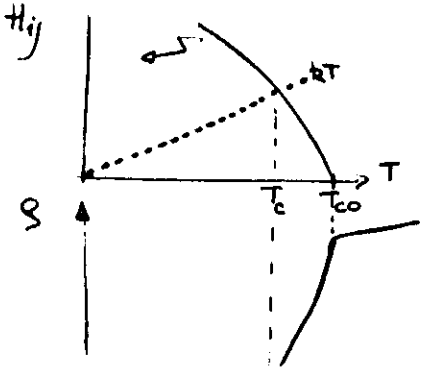

Fig 1' No Meissner Currents

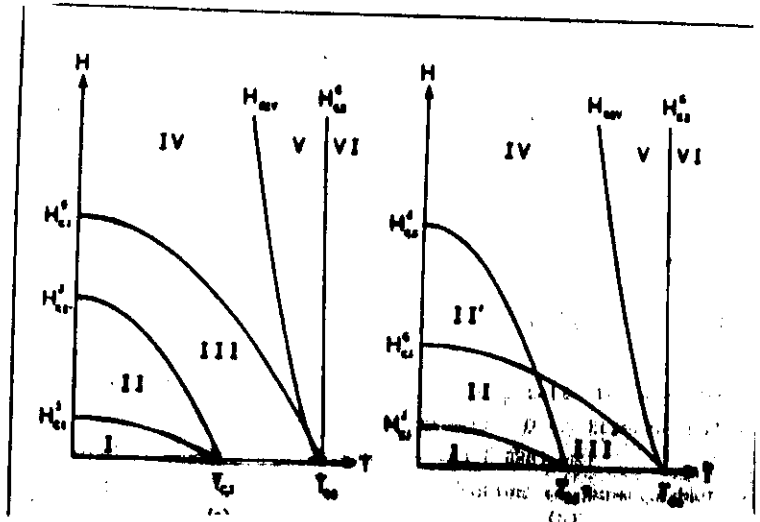

Fig. 2

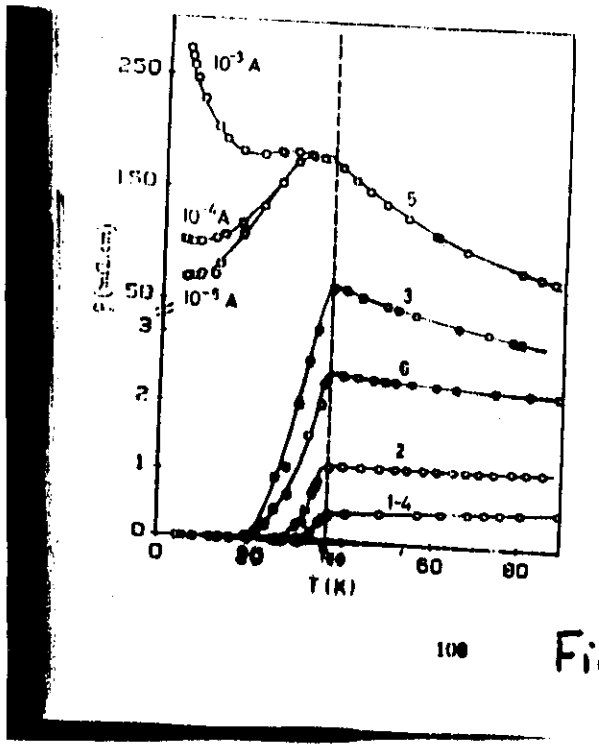

100

Fig 3

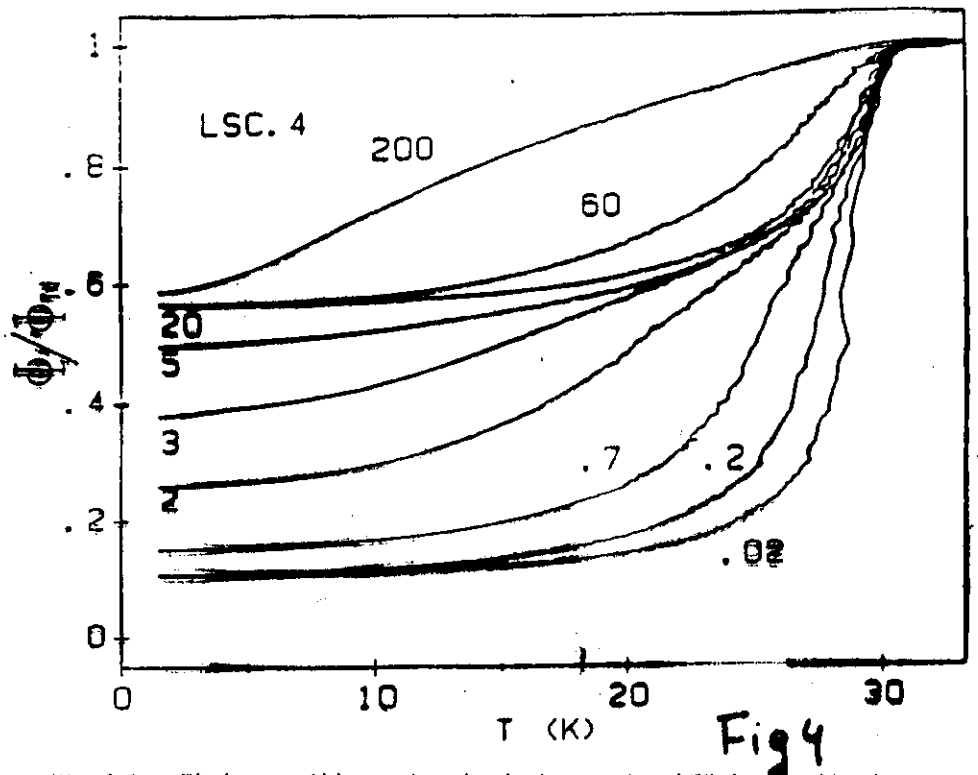

Fig 4

Fig.4.1: Flujo magnético a través de la muestra LSC.4 normalizado por el flujo en el estado normal, como función de temperatura en experimentos ZFC. El número en cada curva indica el campo aplicado en Oe.

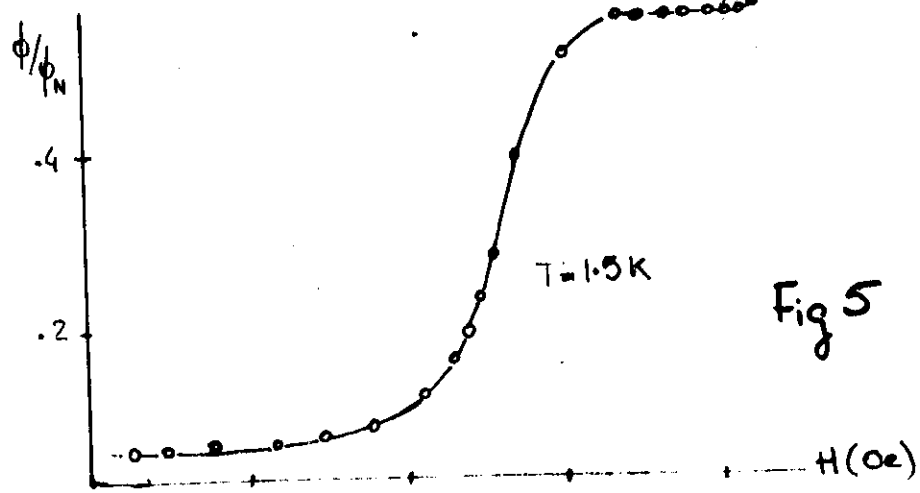

Fig 5

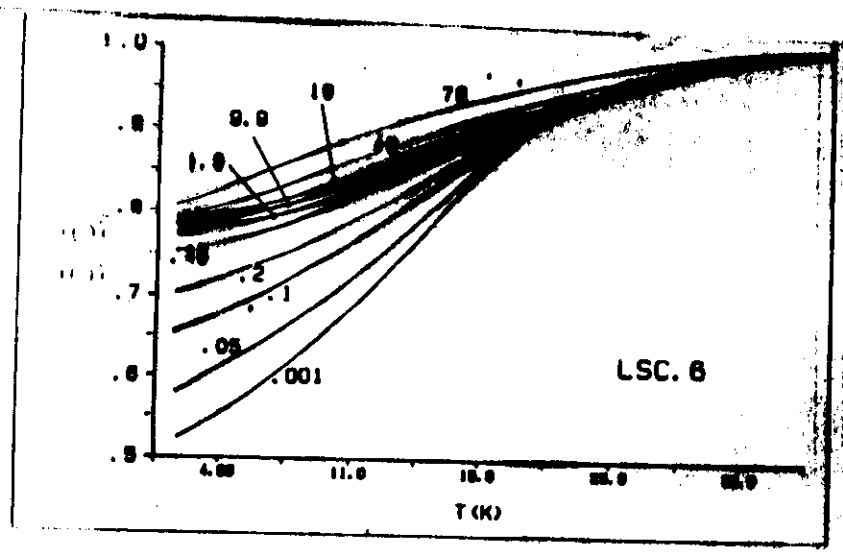

Fig 6

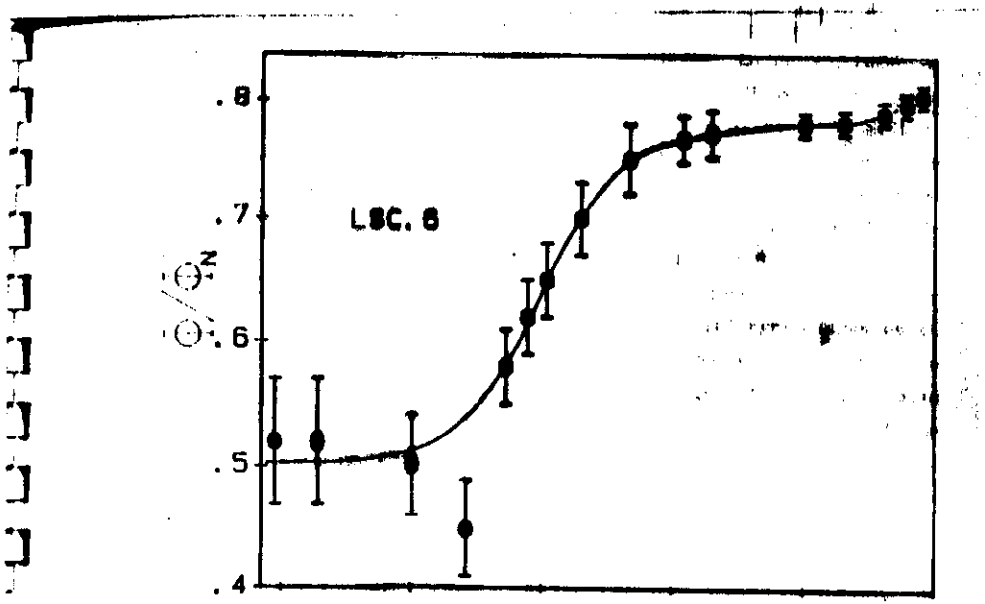

Fig 7

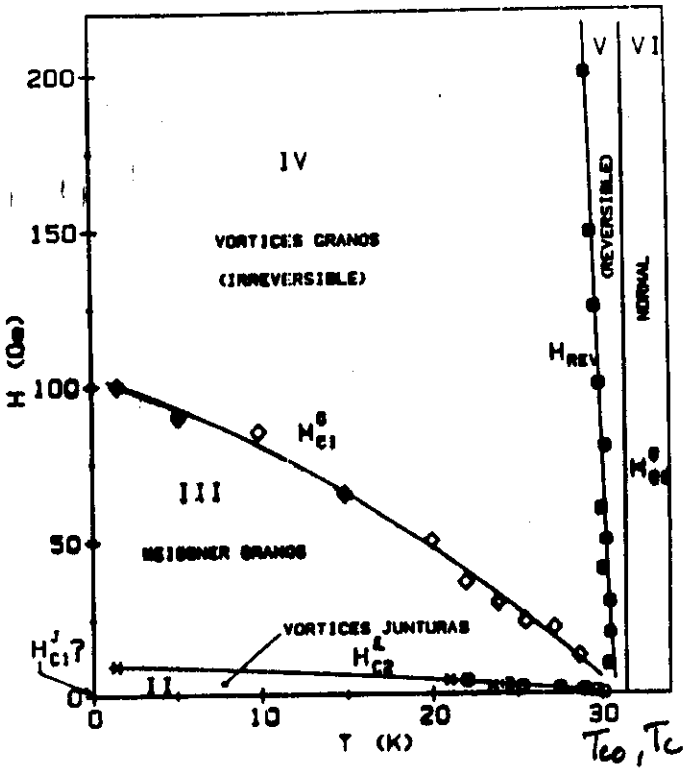
200
150
100
50
0
H (Oe)
IV
VORTICES GRANDES
(IRREVERSIBLE)
III
MEISSNER GRANDE
II
V
VI
REVERSIBLE
NORMAL
H_{REV}
H^0_{c2}
H^0_{c1}
H^J_{c1}?
VORTICES JUNTURAS
H^L_{c2}
0
10
20
30
T (K)
T_{co}, T_c

Fig 8

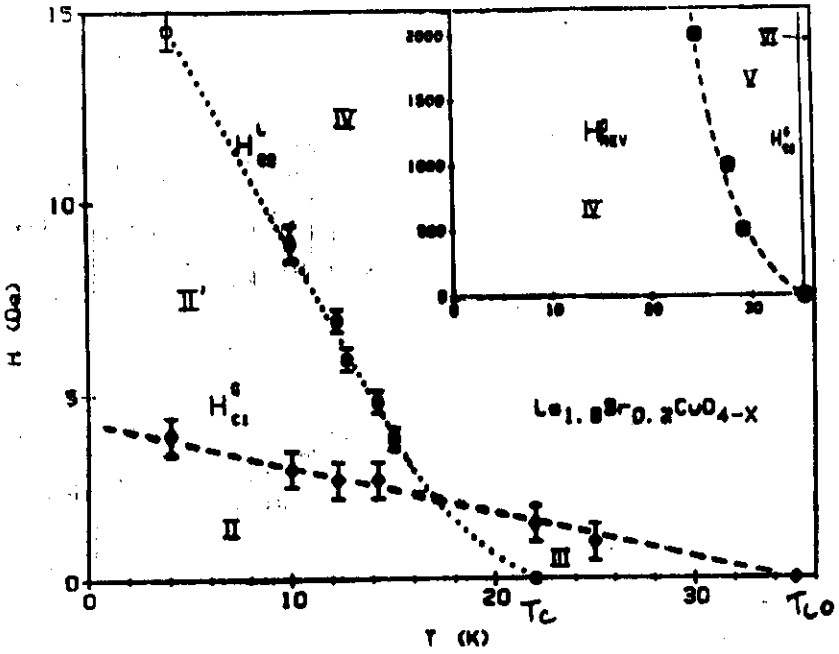
15
10
5
0
H (Oe)
I
II'
II
III
IV
V
VI
H^L_{c2}
H^0_{c1}
H^0_{REV}
H^0_{c2}
$La_{1.8}Sr_{0.2}CuO_{4-X}$
0
10
20
30
T_c
T_{co}
T (K)

Fig 9

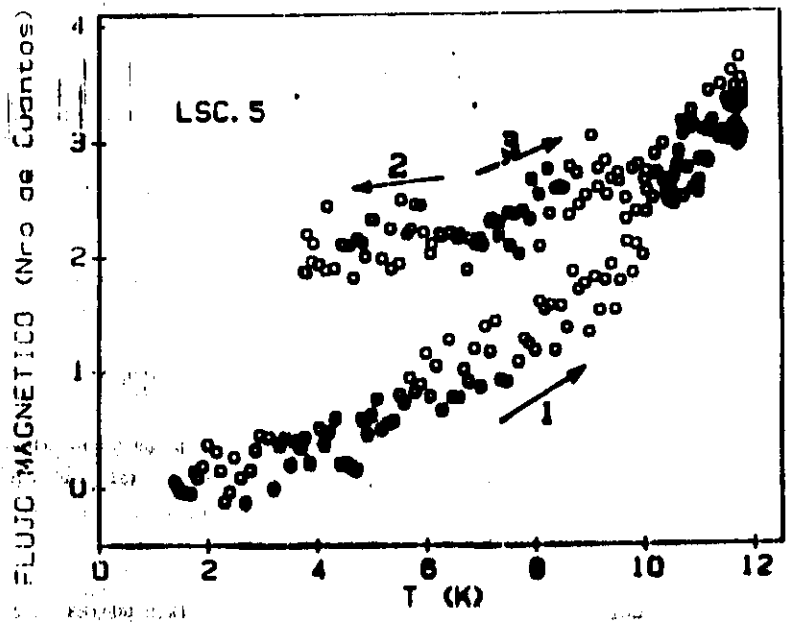
LSC. 5
FLUJO MAGNETICO (Nro de Cuantos)
T (K)
1
2
3

Fig. 10

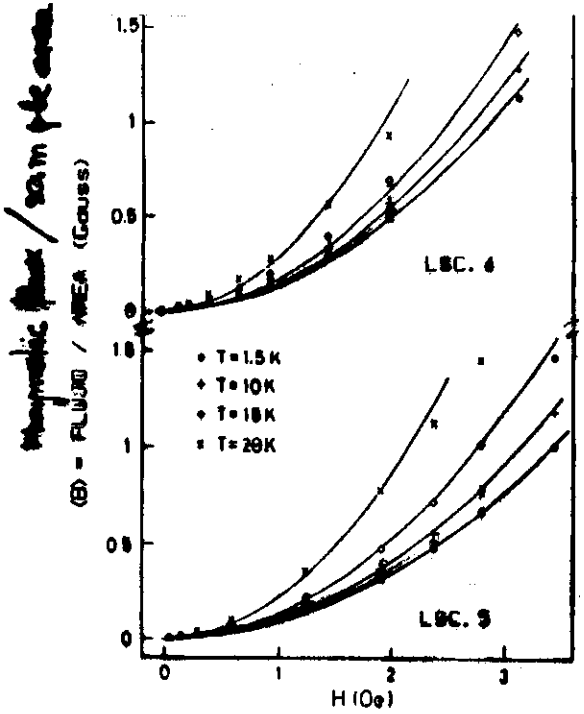
LSC. 4
LSC. 5
T = 1.5 K
T = 10 K
T = 15 K
T = 20 K
H (Oe)

Fig 11

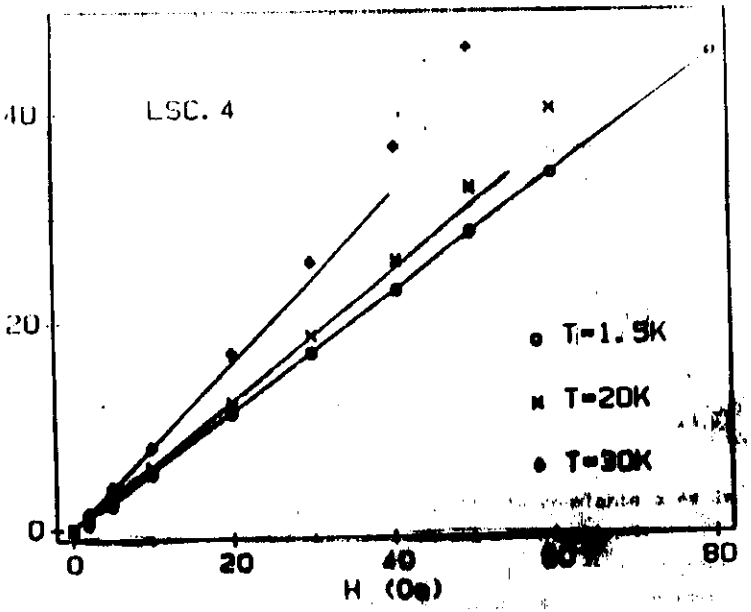

Fig 12

Los valores de H_s obtenidos a partir de (4.7) y estos datos son

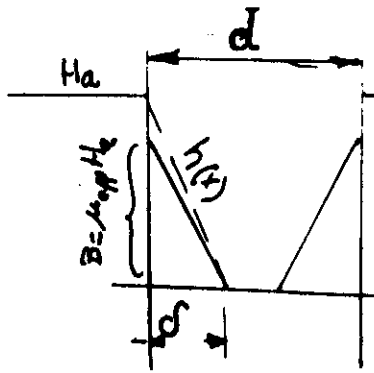

$$\cot h = \frac{dh}{dx} = \frac{4\pi}{c} J_c \neq f(H)$$

$$\delta = \frac{c H_a}{4\pi J_c}$$

if $\delta < \frac{d}{2}$ $\quad \Phi = \frac{c}{8\pi} \frac{(2w+2d)}{J_c} H_a^2$

$\delta = \frac{d}{2}$ $\quad \Phi = \left(H_a - \frac{H_s}{2}\right) A$; 4 rod

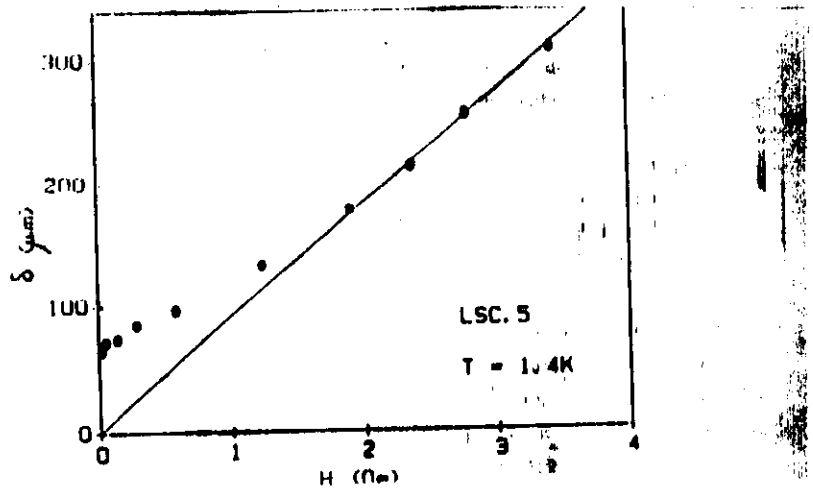

Fig 13

if $\mu_{eff} \neq 1$ $\quad \phi = \frac{c}{8\pi} \frac{P}{J_c} \mu_{eff} H_a^2 \quad \delta < \frac{d}{2}$

$$\phi = \mu_{eff} A \left(H_a - \frac{H_s}{2}\right)$$

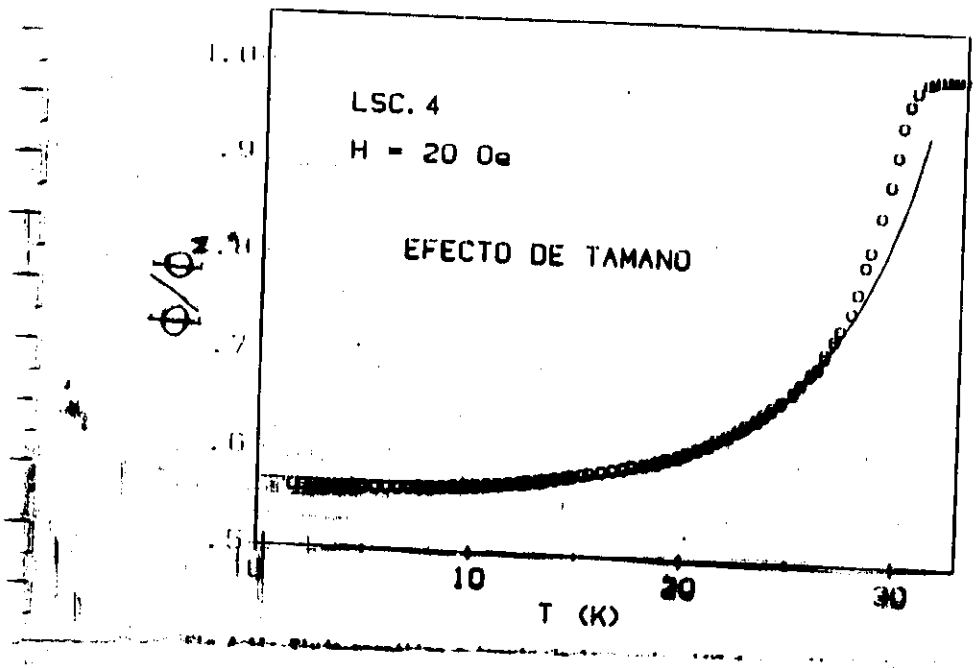

Ajuste:

i) $R \sim 1\mu m$ $(\lambda(0) \sim 3000 Å)$

ii) $\eta \sim .8$

Fig 14

$$\Phi = A H_a \left[1 - \frac{3}{8} \eta f(R/\lambda(T))\right]$$

$$f(R/\lambda) = \left[1 - \frac{3\lambda(T)}{R} \coth \frac{R}{\lambda(T)} + 3\frac{\lambda^2(T)}{R^2}\right]$$

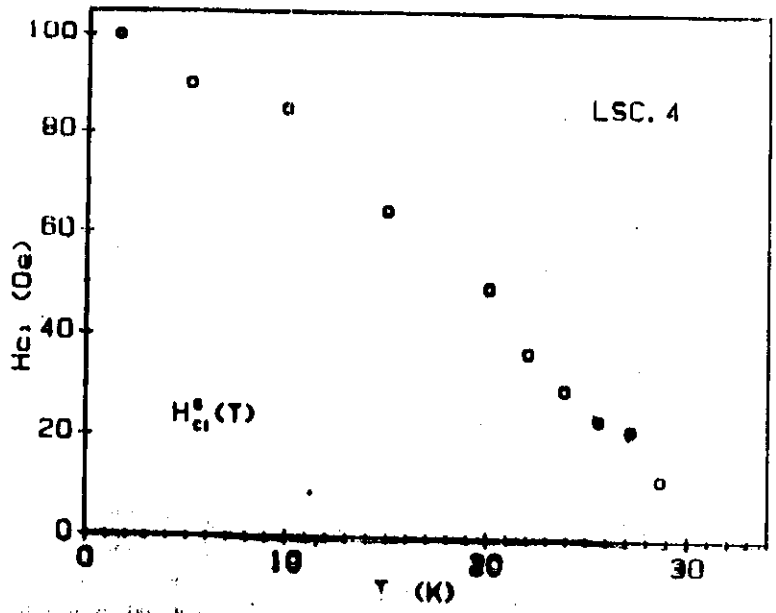

Fig. 4.10: Campo crítico inferior de los granos de la muestra LSC. 4.

Fig 15

$$H_{c1} = \frac{\phi_0}{4\pi\lambda^2} (\ln \kappa)$$

Tentative Phase Diagram of a Ceramic Superc.

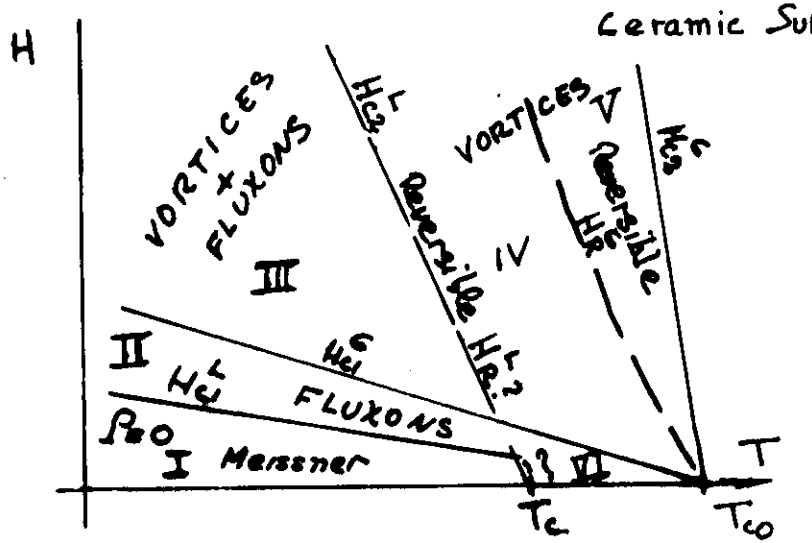

Experimental

I $\rho = 0$; $\Delta \underline{\Phi} \simeq H$ and reversible in T, no RM

II $\rho = 0$; $\Delta \underline{\Phi} \neq H$ and non reversible, RM $\Rightarrow$ 0 at T_c

III $\rho = 0$; $\Delta \phi \neq H$ and no revers., RM $\Rightarrow$ 0 in T_c

IV $\rho \neq 0$; $\Delta \phi \neq H$ " " " " $\Rightarrow$ 0 " "

V $\rho \neq 0$; $\Delta \phi \neq H$ but reversible, RM $\Rightarrow$ 0 in T_c

VI $\rho \neq 0$; $\Delta \underline{\Phi} \simeq H$, Islands in Meissner S

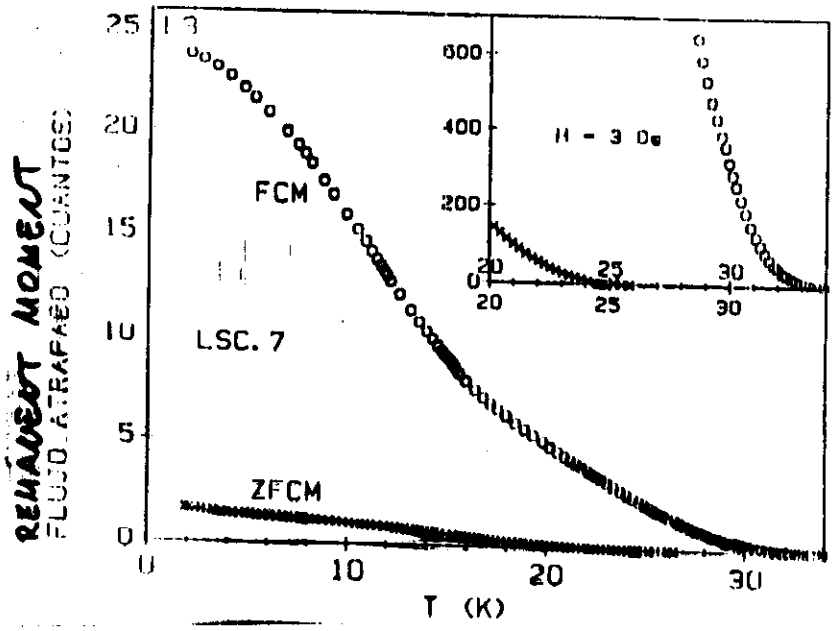

L. Civale et al. Mod Phys. Lett. B3, 173(1989)

Ceramics : Conclusions

1) Granular behavior : Islands smaller than ceramic grains

2) Small coherence length: necessary but not sufficient condition

3) Non superconducting matrix : of unknown origin . Correlated defects

4) Granularity and normal properties : The insulating barriers are Josephson barriers for pairs and tunneling barriers for single particles

$$\rho = \frac{m^*}{ne^2}\left(\frac{1}{\tau_e} + \frac{1}{\tau_i}\right)$$

$$\frac{1}{\tau_e} = \frac{1}{\tau_e^a} + \frac{1}{\tau_e^b}$$

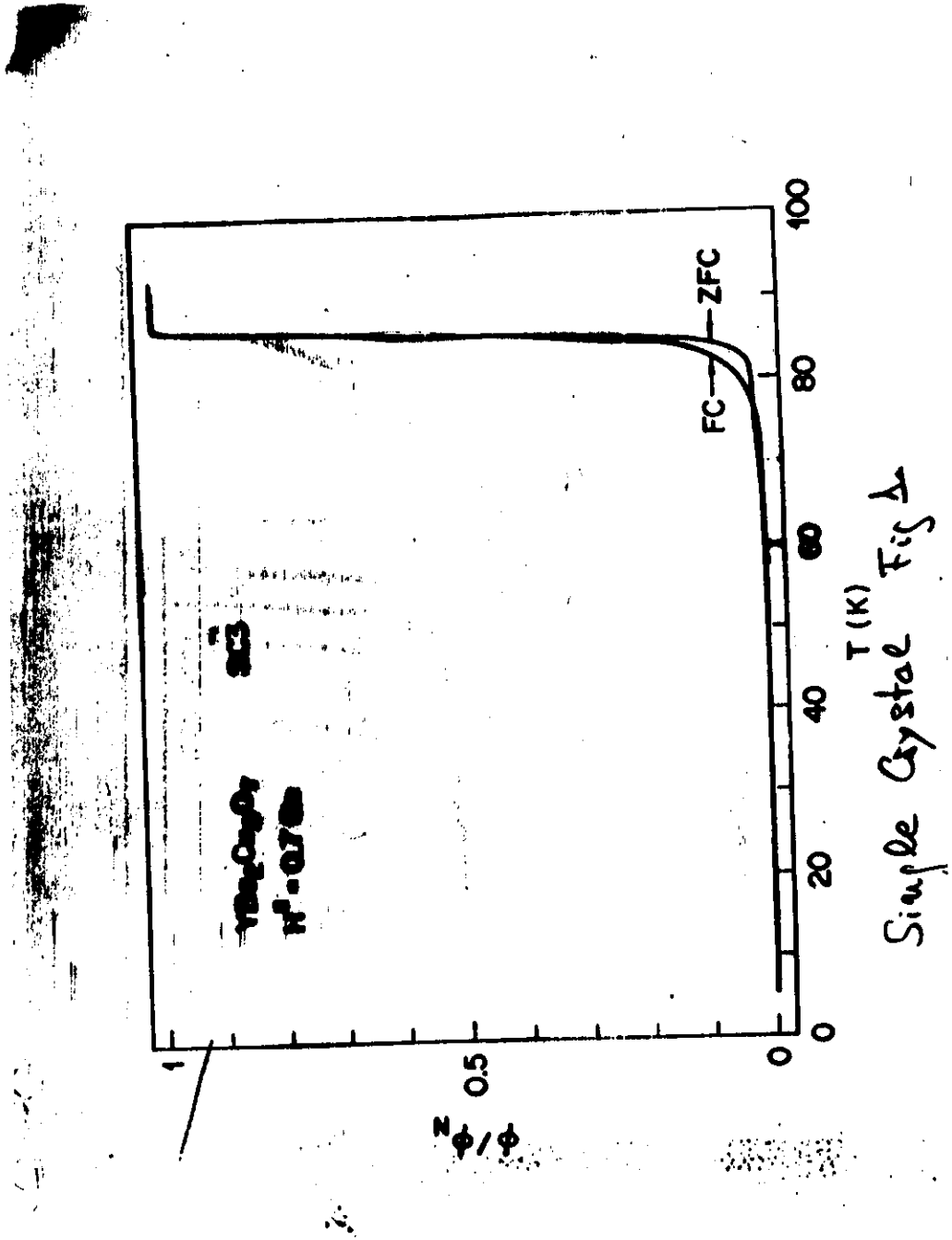

Single Crystal Fig 1

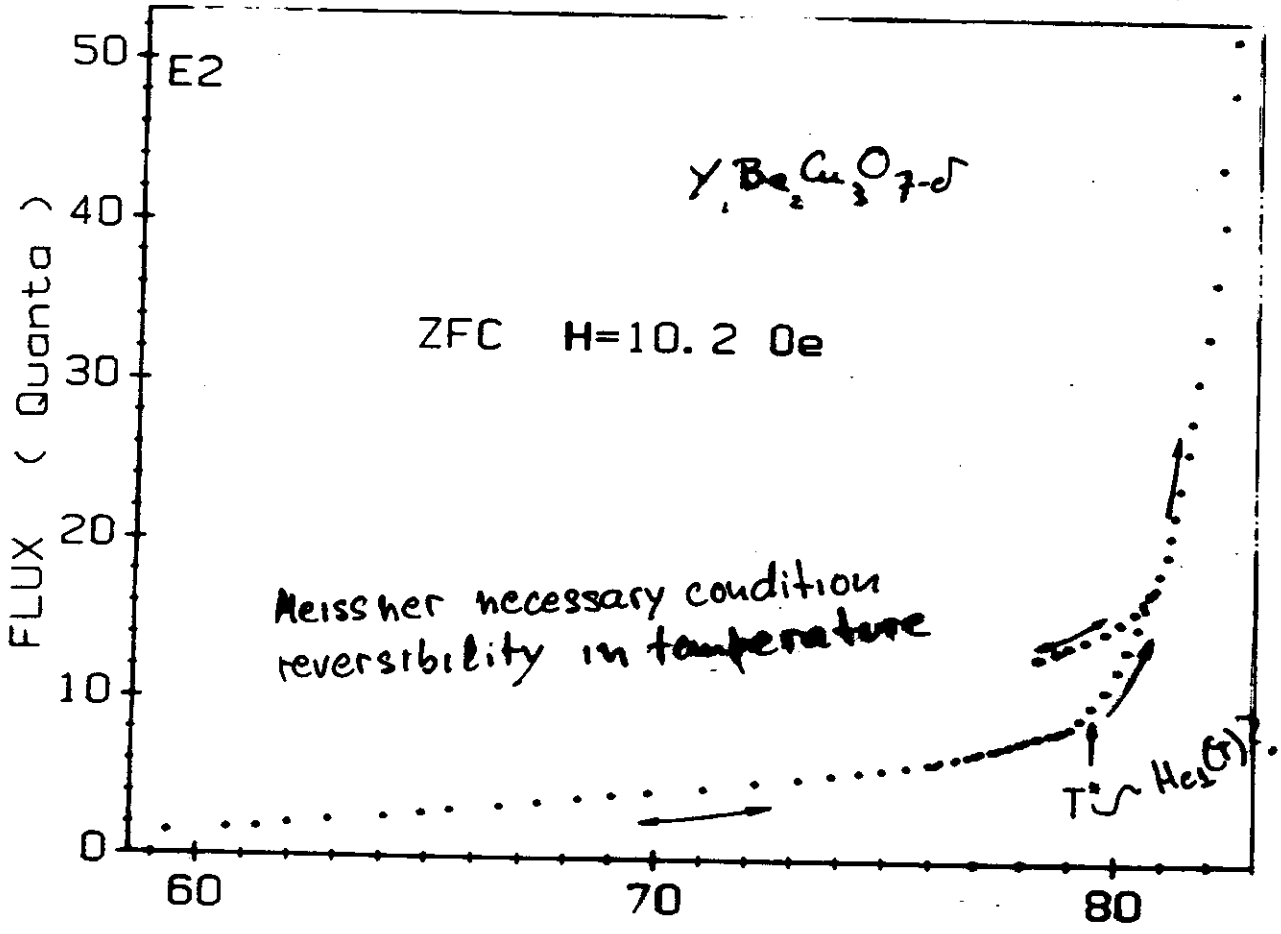

Simple Crystal Fig 1'

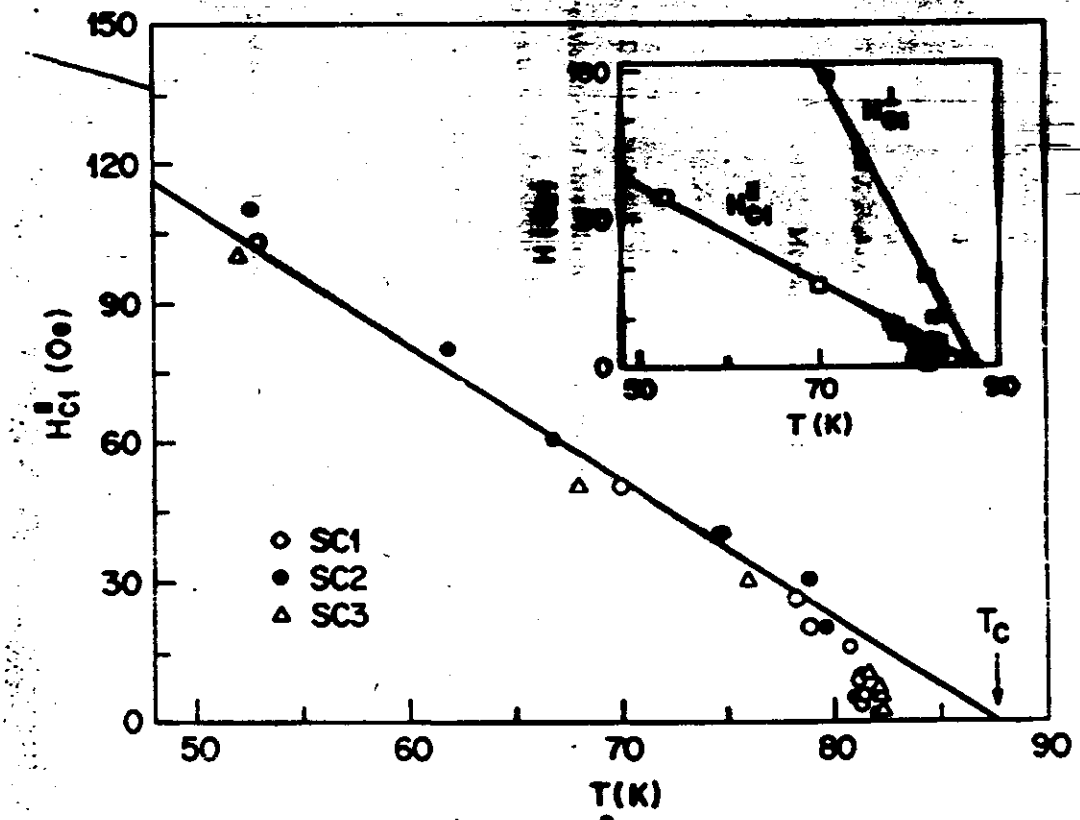

Simple crystals fig 2

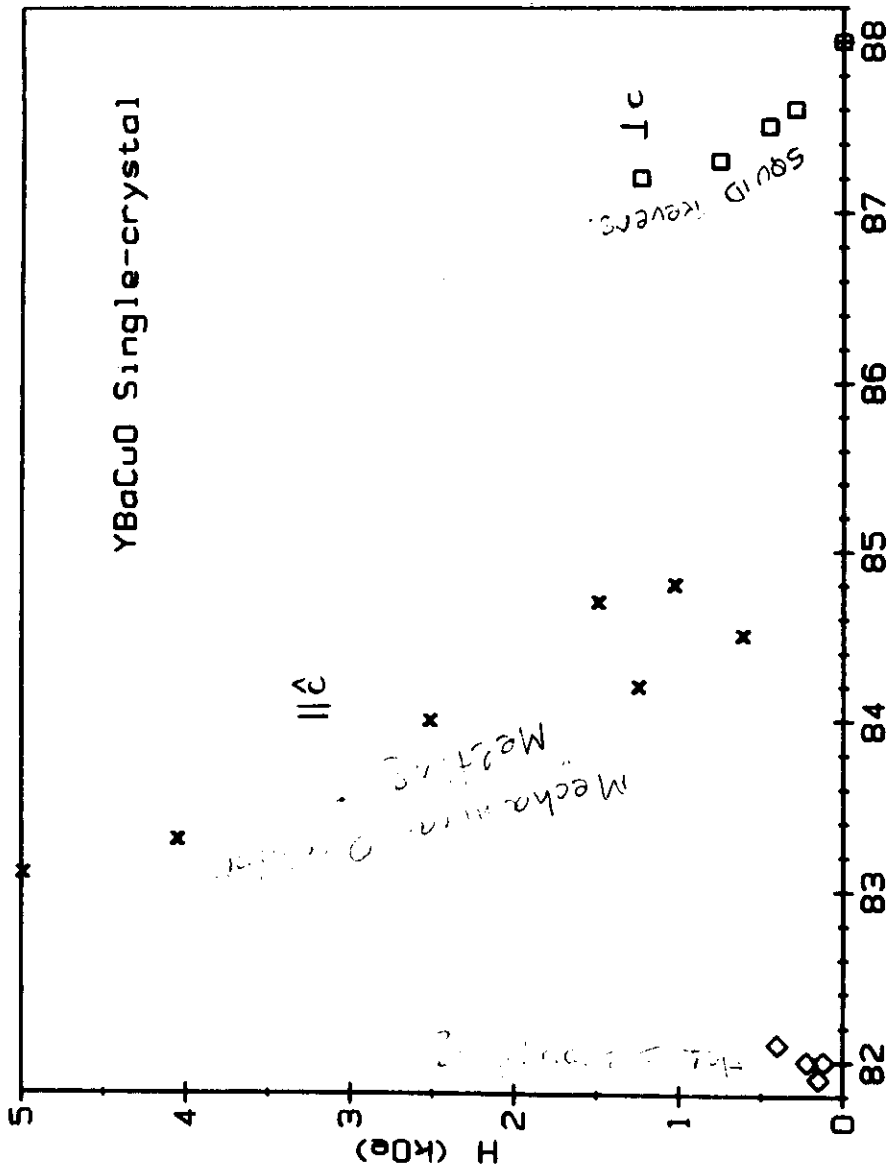

FIG. 4

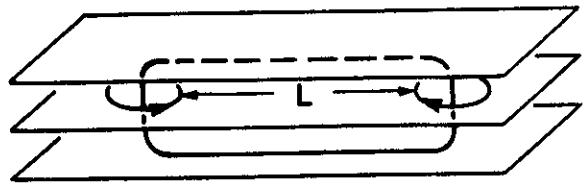

Fig.8: A two-dimensional vortex loop of size L.

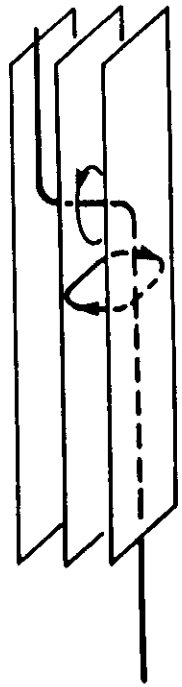

Fig.9: Kink motion of a vortex with core parallel to the planes.

FIG. 3

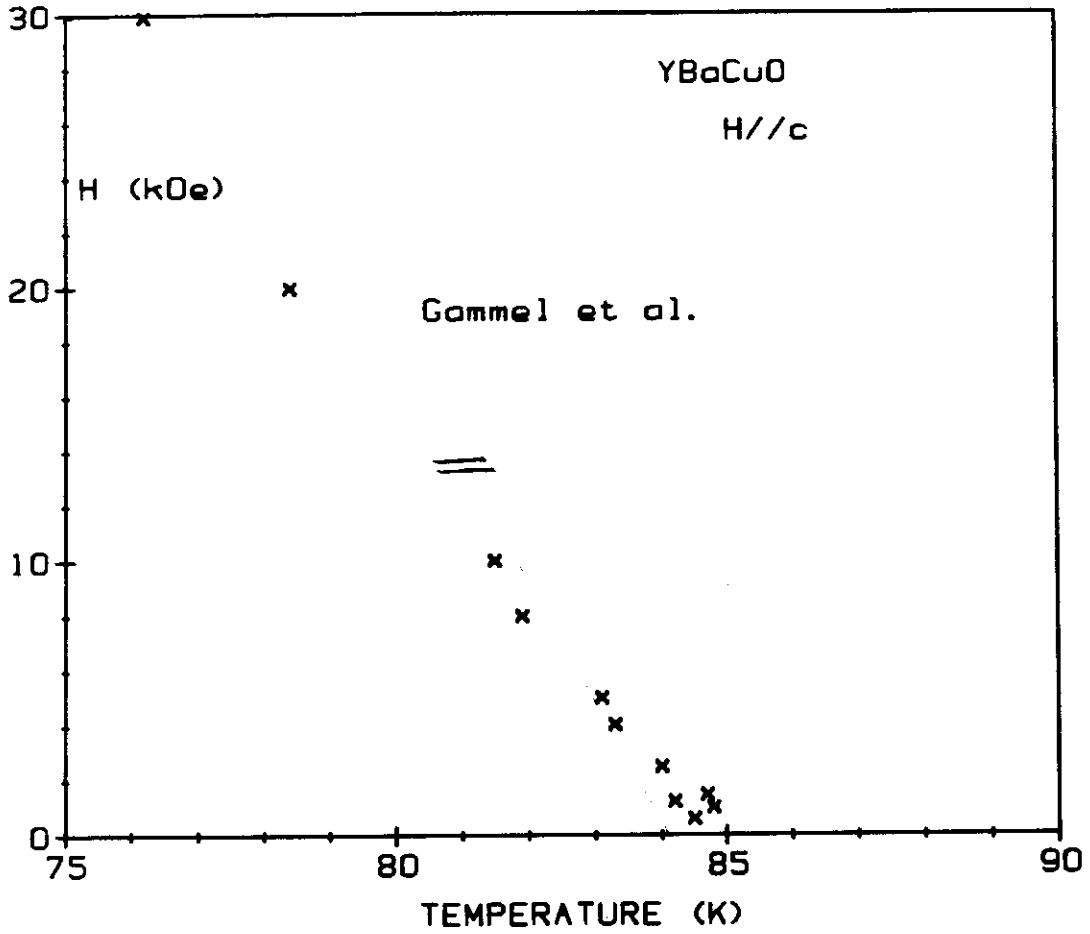
YBaCuO
H//c
H (kOe)
Gammel et al.
30
20
10
0
75
80
85
90
TEMPERATURE (K)

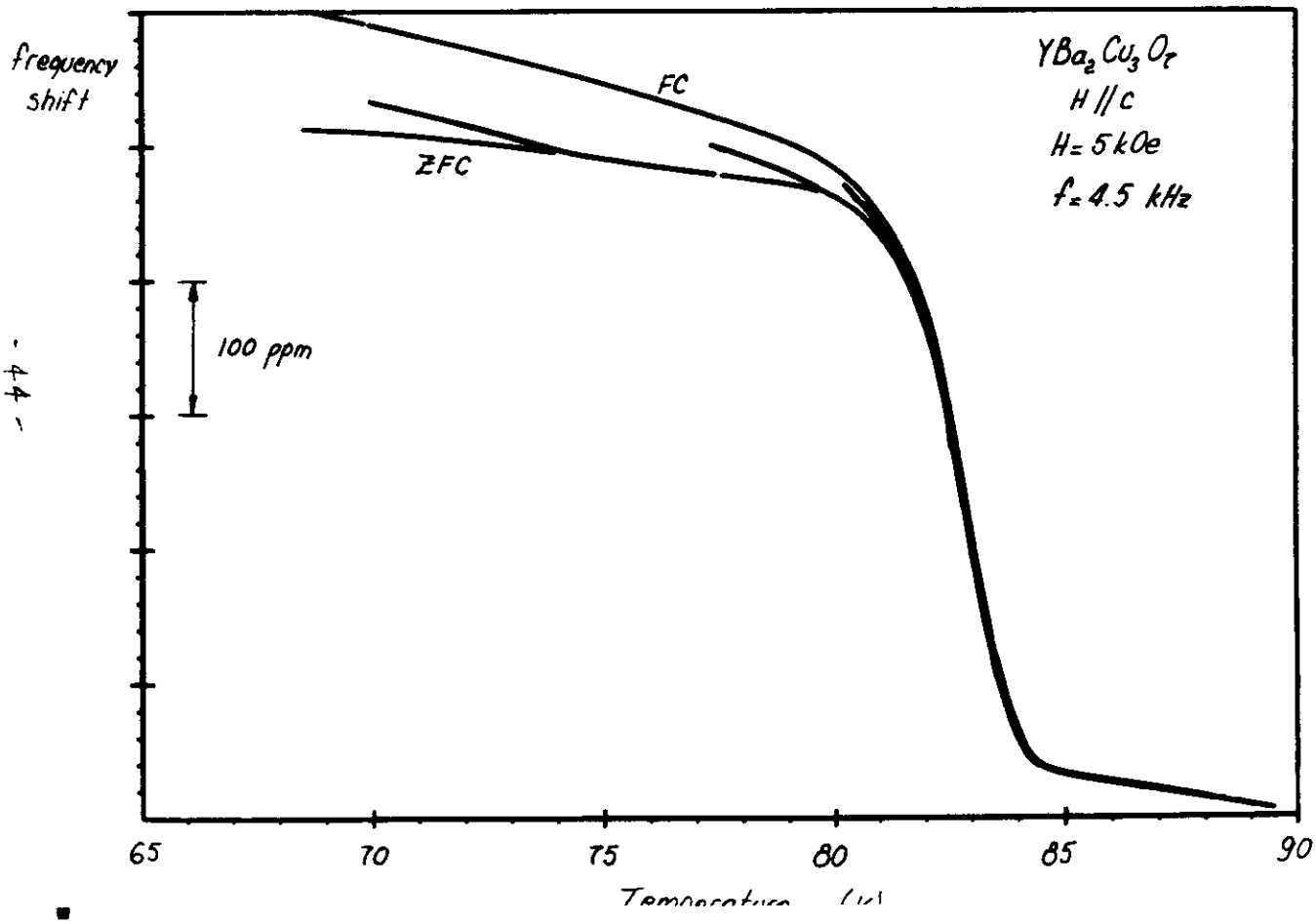
frequency shift
FC
ZFC
100 ppm
$YBa_2Cu_3O_7$
H // c
H= 5 kOe
f= 4.5 kHz
65
70
75
80
85
90

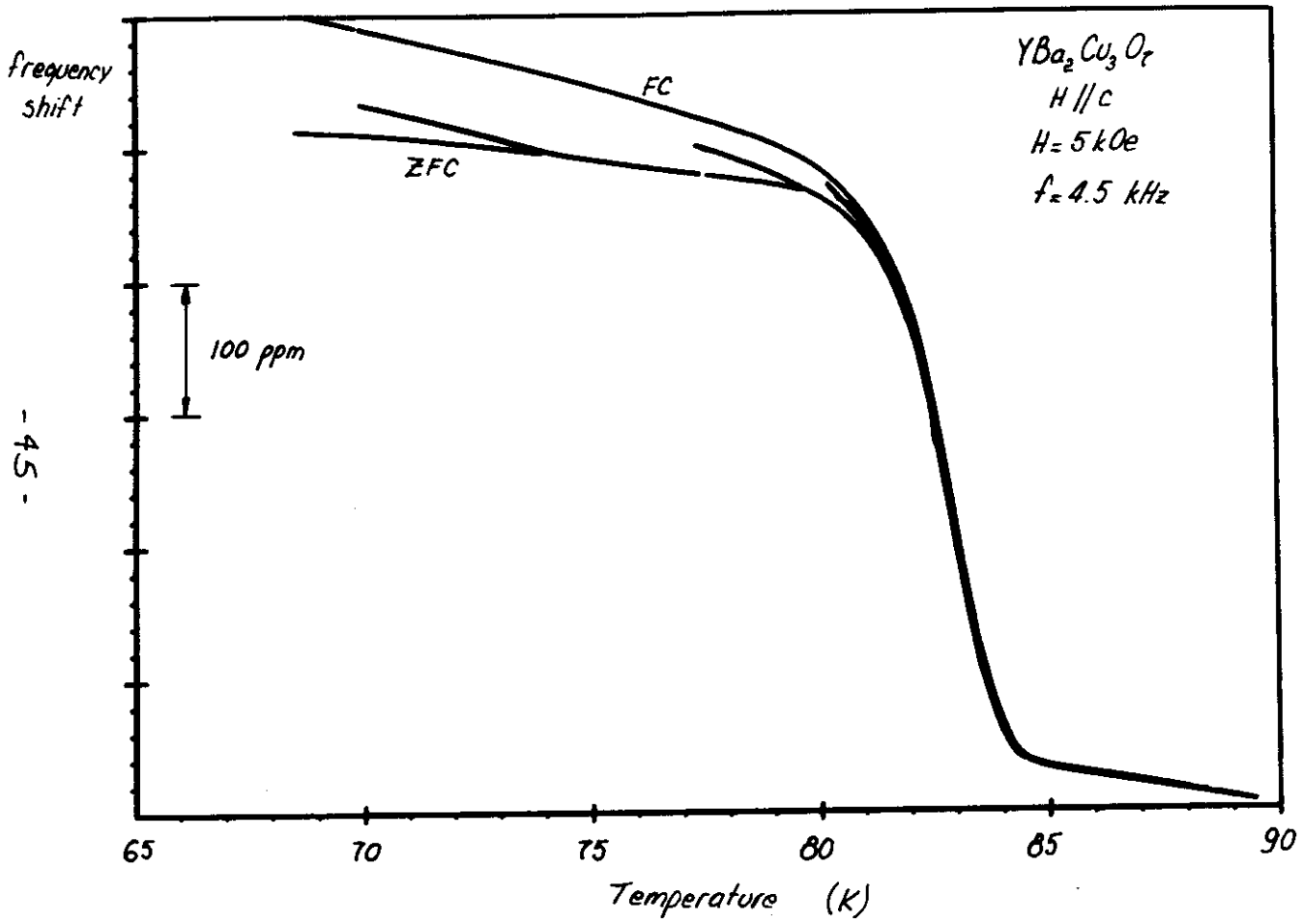
Frequency shift
FC
ZFC
100 ppm
$YBa_2Cu_3O_7$
H // c
H = 5 kOe
f = 4.5 kHz
65
70
75
80
85
90
Temperature (K)